Int J Earth Sciences (Geol Rundsch) (2001) 90:77–87
DOI 10.1007/s005310000152

ORIGINAL PAPER

Greg Hirth · Christian Teyssier · W. James Dunlap

An evaluation of quartzite flow laws based on comparisons between experimentally and naturally deformed rocks

Received: 22 November 1999 / Accepted: 9 October 2000 / Published online: 23 March 2001

Abstract We use the remarkable similarity between microstructures preserved in naturally and experimentally deformed quartzites as a basis to evaluate quartzite flow laws and their application to natural conditions. The precision of this analysis is relatively high because of the well-constrained deformation history of naturally deformed rocks from the Ruby Gap duplex, Central Australia. The external state variables during deformation in the duplex are well constrained by a combination of thermochronological, microstructural and structural observations. Using a flow law with the form $\dot{\varepsilon} = A f_{H_2O}^m \sigma^n \exp(-Q/RT)$, our analysis indicates that values of log (A)=–11.2±0.6 MPa^{-n}/s and Q=135± 15 kJ/mol provide the best description of the combined natural and experimental constraints with values of m=1 and n=4. Motivated by the results of our analysis, we also evaluated the influence of water fugacity on strain rate determined in the laboratory. In this case, we concur with a previously published suggestion that the measured effect of water fugacity ($\dot{\varepsilon} \propto f_{H_2O}^2$) is likely a manifestation of a change in deformation process with increasing stress. The results of this study provide further support for the application of quartzite flow laws to understand deformation conditions in the Earth, and emphasize the important insights that can be gained by analyzing deformation microstructures in naturally deformed rocks.

Keywords Flow laws · Microstructure · Quartzite · Recrystallization · Rheology

G. Hirth (✉)
Department of Geology and Geophysics,
Woods Hole Oceanographic Institution, Woods Hole,
MA 02543, USA
E-mail: ghirth@whoi.edu
Phone: +1-508-2892776
Fax: +1-508-4572183

C. Teyssier
Department of Geology and Geophysics,
University of Minnesota, Minneapolis, MN 55455, USA

W.J. Dunlap
Research School of Earth Sciences,
Australian National University, ACTON, ACT 0200,
Australia

Introduction

Because of the abundance of quartz-bearing rocks in the continental crust, microstructural analyses of quartz and quartzite are important for understanding a wide range of problems in structural geology (e.g., Law et al. 1984; Lister and Snoke 1984; Hacker et al. 1990; Dunlap et al. 1997). In addition, the rheological properties of quartzite have been used to constrain a variety of geodynamic properties of the crust, including the depth extent of the seismogenic zone (e.g., Sibson 1977; Hobbs et al. 1986), the strength of the crust (e.g., Kohlstedt and Weathers 1980; Ord and Christie 1984), and time-dependent "stress-triggering" of earthquakes (e.g., Freed and Lin 1998). Microstructural observations have also been combined with independent estimates of temperature and pressure to compare deformation mechanisms operative in the crust with predictions based on experimental studies (e.g., Dresen et al. 1997; Stockhert et al. 1999; Stipp et al. 1999). The analyses of Dresen et al. (1997) and Stöckhert et al. (1999) indicate that, in general, some experimental quartzite flow laws provide a good description of the rheological properties of the crust.

Despite at least 40 years of study, there are still considerable uncertainties in our understanding of the rheological properties of quartzite. Microstructural observations on both naturally (e.g., McLaren and Hobbs 1972; White 1976) and experimentally (e.g., Carter et al. 1964; Tullis et al. 1973) deformed quartzites have demonstrated that dislocation creep is a dominate deformation mechanism for quartzite. How-

ever, extrapolation of even the best constrained dislocation creep flow laws to natural conditions indicates that large uncertainties in the rheological properties of quartzite remain. For example, when calculating strength versus depth envelopes for thrusting environments in the crust (e.g., Brace and Kohlstedt 1980), the range of differential stresses predicted by published quartzite flow laws exceeds 400 MPa at a depth of ~15 km (e.g., Fig. 10 of Gleason and Tullis 1995).

In this study, we use results from a combination of microstructural, geochronological and geological observations to provide additional constraints on the flow law parameters for quartzites. The analysis is motivated by the observation that microstructures preserved in quartz mylonites from the Ruby Gap duplex, central Australia, indicate that the three dislocation creep regimes identified in the laboratory (Hirth and Tullis 1992) also occur under natural conditions (Dunlap et al. 1997). The positive correlation between the naturally and experimentally produced microstructures indicates that the flow laws determined in the laboratory are representative of deformation processes that occur in the Earth.

The rheological properties of quartzite are analyzed using the flow law:

$$\dot{\varepsilon} = A f_{H_2O}^{m} \sigma^{n} \exp(-Q/RT) \quad (1)$$

where $\dot{\varepsilon}$ is strain rate, A is a material parameter, f_{H_2O} is water fugacity, m is the water fugacity exponent, σ is differential stress, n is the stress exponent, Q is the activation energy, R is the ideal gas constant, and T is absolute temperature. There is significant variation in the value of these parameters determined by experiments (e.g., Paterson and Luan 1990, see Table 1; Gleason and Tullis 1995, see Table 3). However, as discussed below, if only the highest stress resolution data are analyzed, specifically, those acquired using a gas apparatus (e.g., Heard and Carter 1968; Luan and Paterson 1992) or liquid confining medium (Gleason and Tullis 1995), several consistencies are apparent. In the remainder of this paper we sometimes use the following abbreviations: H&C (Heard and Carter 1968); L&P (Luan and Paterson 1992); G&T (Gleason and Tullis 1995).

The highest resolution experimental studies show similarities in the values of n, Q, and the effect of water on strain rate. The value of $n \approx 4$, determined for both the "melt-present" and "melt-free" flow laws of G&T), is the same as that determined for the "silicic-acid origin" samples of L&P. Similar values of Q were also determined in these studies, but the range in Q (137±34 kJ/mol for the "melt present" flow law of G&T, 152±71 kJ/mol for the "silicic-acid origin" samples of L&P, and 223±56 kJ/mol for the "melt free" flow law of G&T) is large enough to result in considerable uncertainty in estimated rheological properties of the crust. For example, using values of Q ranging from 130–220 kJ/mol, an extrapolation from 900 (lab. conditions) to 300 °C at a constant stress and water fugacity indicates more than four orders of magnitude uncertainty in strain rate. Experimental evidence suggests that the influence of water on strain rate can be described by a pre-exponential, power law water fugacity term (e.g., Paterson 1989; Gleason and Tullis 1995; Kohlstedt et al. 1995). However, the value of the water fugacity exponent (m) in Eq. (1) has been calculated to be ~1 (Gleason and Tullis 1995; Kohlstedt et al. 1995), ~2 (Post et al. 1996), or ~2.7 (Paterson, see personal communication in Post et al. 1996). As described below, quantification of the effect of water is complicated by the fact that the experiments of Gleason and Tullis (1995) and Heard and Carter (1968) may not have been conducted at water saturated conditions and therefore the water fugacity was not well constrained.

Quartzite microstructures in the Ruby Gap duplex

Microstructures preserved in quartz mylonites from the Ruby Gap duplex indicate that the three dislocation creep regimes identified in experimental studies (Hirth and Tullis 1992) also operate in the Earth, indicating that deformation processes operating under natural conditions are the same as those activated in the laboratory (Dunlap et al. 1997; Hirth et al. 1998). The distinctive microstructures that characterize each regime are produced primarily by the operation of different mechanisms of dynamic recrystallization (Hirth and Tullis 1992). Micrographs of quartz mylonites from the Ruby Gap duplex exhibiting microstructures characteristic of the three dislocation creep regimes are shown in Fig. 1. The duplex is comprised of a 3-km-thick antiformal stack of six superposed thrust sheets that formed under greenschist facies conditions. Maps and cross sections showing details of how the quartzite microstructures vary in the duplex are given in Dunlap et al. (1997).

In sheet 1 of the duplex (the lowest of six sheets that define the thrust system), the grains exhibit irregular patchy extinction, numerous deformation bands, and extremely fine recrystallized grains along the grain boundaries (Fig. 1a). In some cases, deformation lamellae are also observed (Fig. 1a). These microstructures are characteristic of regime 1, where dislocation climb is difficult and recrystallization occurs by grain boundary migration [often referred to as grain boundary bulging (e.g., Bailey and Hirsch 1962)].

Moving upward in the thrust system, abrupt transitions in the quartz microstructure are observed between the major thrust sheets. In sheet 2, the original quartz grains are extremely flattened and exhibit optically visible subgrains, as well as recrystallized grains along their boundaries (Fig. 1b). These microstructures are characteristic of regime 2, where recovery is accommodated by dislocation climb and recrys-

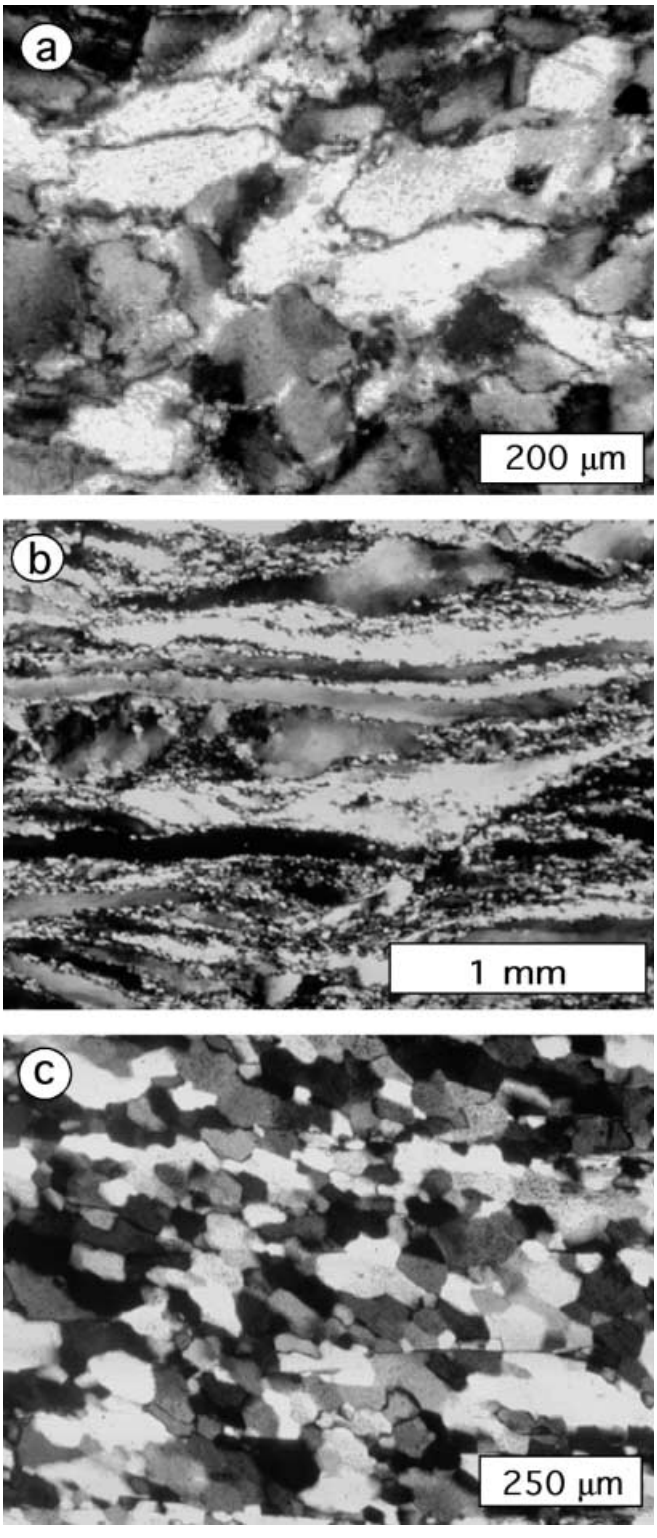

Fig. 1 Optical micrographs of quartz mylonites from the Ruby Gap duplex. **a** Regime 1 microstructure showing grains with patchy extinction, deformation bands and fine recrystallized grains along the grain boundaries. Deformation lamellae are present in some grains. **b** Regime 2 microstructure showing extremely flattened original grains exhibiting optically visible subgrains. The core and mantle texture, in addition to the similarity in size of recrystallized grains and subgrains, are characteristic of subgrain rotation recrystallization. **c** Regime 3 microstructure characterized by complete recrystallization and oblique foliation indicative of grain boundary migration recrystallization. All micrographs in cross-polarized light

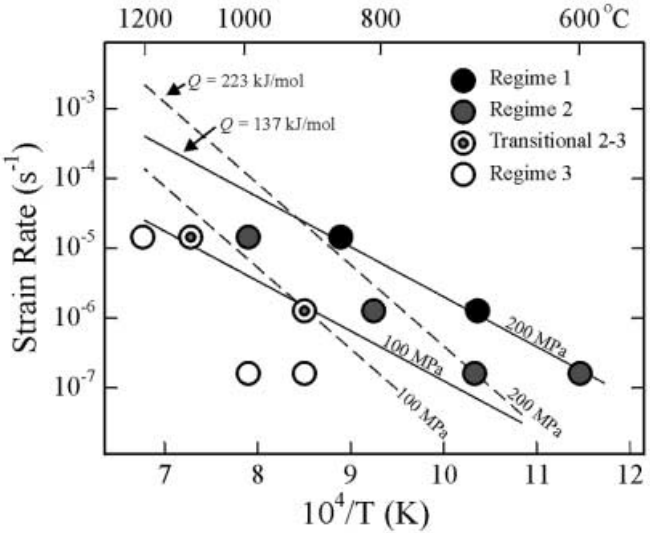

Fig. 2 Plot of log strain rate versus 1/T showing experimental conditions where dislocation creep regimes are observed for "as-received" quartzites (after Hirth and Tullis 1992). Also shown are contours of constant stress calculated using the "melt" (*solid lines*) and "no-melt" (*dashed lines*) quartzite flow laws of Gleason and Tullis (1995)

tallization occurs dominantly by progressive subgrain rotation.

In sheets 3 through 6 the quartzite is completely recrystallized, and exhibits an oblique foliation defined by the recrystallized grains (Fig. 1c). This microstructure is characteristic of regime 3, where recovery is accommodated by dislocation climb, and recrystallization occurs dominantly by grain boundary migration.

The transitions between dislocation creep regimes occur with decreasing stress from regime 1 (highest stress) to regime 3 (lowest stress). Accordingly, the transitions are observed to occur in the laboratory with changes in temperature, water fugacity, or strain rate. The experimental conditions where these transitions were observed by Hirth and Tullis (1992) for "as-received" quartzite are illustrated in Fig. 2. To provide an estimate of the stresses at which the transitions occur, lines of constant differential stress are plotted on Fig. 2 using the Gleason and Tullis (1995) flow laws. The G&T flow laws were determined for conditions where climb-controlled creep was interpreted to be the deformation mechanism based on a combination of microstructural observations and the observed flow law parameters (Gleason and Tullis 1995). Therefore, the extrapolation of these flow laws to stresses above ~200 MPa, where the transition to regime 1 is observed, is not valid because it is likely that the rate-controlling step in the deformation proc-

ess changes. We return to this important constraint later in the paper when we discuss the role of water fugacity on creep rate. The G&T flow laws indicate that the stress at the transition between regimes 1 and 2 is approximately a factor of two greater than that at the transition between regimes 2 and 3.

Input variables based on geological analysis of the Ruby Gap duplex

The relatively simple tectonic history of the Ruby Gap duplex, the similarity between experimentally and naturally produced microstructures, and the well constrained thermal history of the duplex (Dunlap et al. 1995; Dunlap 1997) provide the opportunity to "test" quartzite flow laws. Here we describe how each of the external state variables (T, σ, $\dot{\varepsilon}$, f_{H_2O}) in the flow law [Eq. (1)] are constrained using data from the Ruby Gap duplex.

Temperature

The temperature during deformation of quartzite in the Ruby Gap duplex is well constrained by thermochronological analyses. A comparison of Ar^{40}/Ar^{39} ages determined for detrital and synkinematically crystallized white micas from the duplex demonstrates that deformation occurred below the closure temperature for Ar exchange (Dunlap et al. 1991. 1995). The current estimate for the closure temperature for Ar exchange in white mica is ~350 °C (e.g., Purdy and Jäger 1976; Hames and Bowring 1994). Thermal modeling based on laboratory diffusion studies on K-feldspar grains from the duplex suggests that the temperature during deformation remained between ~250±20 and 330±20 °C (Dunlap 1997).

Differential stress

The differential stress during deformation is constrained using recrystallized grain size piezometry, as well as the identification of the transitions between dislocation creep regimes. For the purposes of this section, we initially limit our analysis to determining the differential stress at the transition between regimes 2 and 3. As illustrated in Fig. 2, the transition between regimes 2 and 3 in the laboratory is observed at a differential stress of ~100 MPa. There is some uncertainty inherent in extrapolating this value to natural conditions. The transition to regime 3 is interpreted to occur because of an increase in the relative velocity of grain boundary migration (Hirth and Tullis 1992). Because the processes that create the driving force and control the mobility of grain boundary migration do not necessarily have the same activation energies (e.g., Derby and Ashby 1987; Shimizu 1998; De Bresser et al. 2000) the transition from regime 2 to regime 3 may occur at a different stress at natural conditions.

The differential stress during deformation in the duplex can also be estimated by analyzing grain sizes in samples that exhibit microstructures transitional between regimes 2 and 3 in the duplex. These samples have recrystallized grain sizes of ~40 μm (see Fig. 7 of Dunlap et al. 1997), consistent with a differential stress of ~60 MPa if the recrystallized grain size piezometer of Twiss (1977) is applied. Experimental observations indicate that the Twiss (1977) piezometer relationship is accurate at conditions near the transition between regimes 2 and 3 (Gleason and Tullis 1993). The value of 60 MPa based on piezometry should be considered a minimum estimate for the differential stress at conditions near the transition between regimes 2 and 3 because of possible temperature effects on recrystallized grain size piezometers (e.g., De Bresser et al. 2000) and the possibility that the natural samples experienced some post-deformational grain growth.

Further constraints on the magnitude of differential stress at the transition between regimes 2 and 3 in the Ruby Gap duplex are provided by microstructural analysis of quartz mylonites that exhibit unequivocal regime 2 microstructures (e.g., Fig. 1b). The recrystallized grain size in these samples is ~20 μm (Dunlap et al. 1997) and is similar to the subgrain size preserved near the grain boundaries. These observations indicate that recrystallization occurred by subgrain rotation, consistent with the regime 2 microstructure, and suggest that the samples did not experience significant post-deformational grain growth. The differential stress estimated for these samples using the Twiss (1977) piezometer is ~80 MPa. However, because the Twiss (1977) piezometer may overestimate the differential stress when recrystallization occurs by subgrain rotation (e.g., Post and Tullis 1999), the value of ~80 MPa should be considered a maximum value estimated by grain size piezometry. In summary, the combination of rheological constraints and recrystallized grain size piezometry indicates that the differential stress at the transition between regimes 2 and 3 in the Ruby Gap duplex is between ~60 and 100 MPa. It is noteworthy that these values agree very well with those determined in other studies where deformation was interpreted to occur at similar temperatures (e.g., Stockhert et al. 1999).

Strain rate

Strain rate is the most difficult deformation parameter to constrain using structural observations alone. However, because of the relatively simple tectonic history of the Ruby Gap duplex, and the fact that deformation occurred at a temperature low enough for argon to be quantitatively retained by newly crystal-

lized micas, the strain rate can be estimated using a combination of strain analysis and geochronology. The analysis of white mica Ar^{40}/Ar^{39} deformation ages and thermal histories calculated using multi-diffusion-domain modeling of K-feldspar Ar^{40}/Ar^{39} data indicates that deformation in the duplex occurred over ~30 million years (Dunlap et al. 1997). Strain analyses of the mylonites in which regime 2 microstructures are preserved, using both the Fry method (Fry 1979) and the algebraic axial ratio method of Shimamoto and Ikeda (1976), indicate that the magnitude of strain was on the order of 1 (Dunlap 1992). It is almost impossible to estimate strain for the fully recrystallized regime 3 mylonites. If strain was accumulated over the entire deformation history of the duplex these constraints indicate an average strain rate of $\sim 10^{-15}$/s (i.e., ~100% strain in ~30 million years). This value must be considered a minimum estimate because deformation did not necessarily occur continuously in each thrust sheet over the entire duration of the orogeny. Indeed, the variation of mica deformation ages throughout the duplex indicates that "microstructural quenching" occurred over ~30 million years (Dunlap et al. 1997).

Another estimate for the strain rate during deformation in the duplex can be calculated based on a combination of geochronology and larger-scale structural observations. Structural reconstructions of the duplex indicate that the upper plate thrusted over the lower plate at a rate of ~1.5 km/million years during the imbrication of the thrust sheets (Dunlap 1992; Dunlap et al. 1997). Assuming this displacement was accommodated only within the quartzite units of the thrust sheets (which had a total thickness of between 1 and -2 km), the strain rate in the quartzites was $\sim 10^{-14}$/s to 5×10^{-14}/s. Because some of the strain was likely accommodated by displacement on the faults separating the thrust sheets, the value of 5×10^{-14}/s gives an estimate for the maximum average strain rate during duplex formation.

Water fugacity

We estimate a maximum value for the water fugacity during deformation by assuming that water was present at a temperature of 300 °C and pressure of ~400 MPa (i.e., the lithostatic pressure at a depth of ~15 km, using a geothermal gradient of ~20 °C/km). The presence of water during deformation is indicated by the observation of synkinematic mica crystallization and abundant fluid inclusions within the original quartz grains. A f_{H_2O} of ~37 MPa was calculated for these conditions using standard water fugacity coefficients (Tödheide 1972).

Extrapolation of quartzite flow laws

Without considering the effects of differences in water fugacity between laboratory experiments and the Earth, extrapolation of even the best constrained quartzite flow laws indicates significant uncertainty in the rheological properties of quartzite at lower greenschist grade conditions. The influence of temperature on the strain rate predicted by the G&T and L&P flow laws at a differential stress of 100 MPa is illustrated in Fig. 3a. The experimental data of G&T and L&P shown in this figure were normalized to a differential stress of 100 MPa using n=4. However, no correction was made for differences in water fugacity between the experimental conditions and the Ruby Gap duplex. Taken at face value, these flow laws provide a loose bracket on the estimated deformation conditions in the Ruby Gap duplex.

To further constrain the parameters of a generalized quartzite flow law we first assume that the difference between the L&P and G&T data sets is the pres-

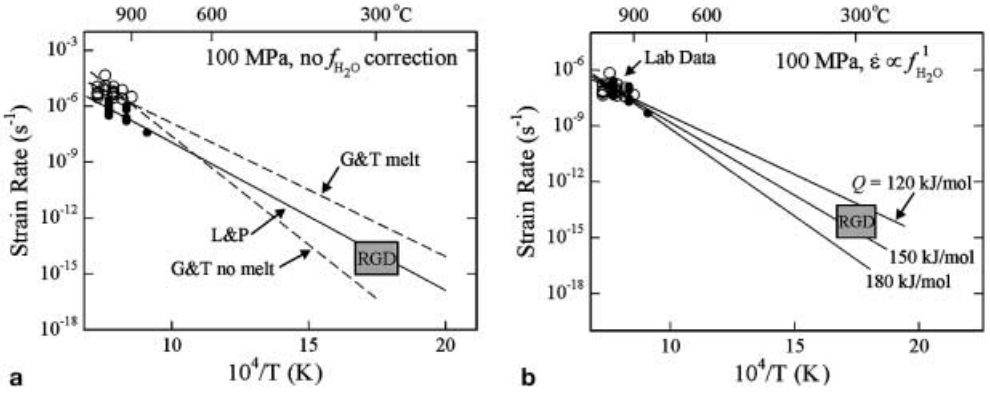

Fig. 3 Plots of log strain rate versus 1/T showing extrapolation of flow laws from experimental to natural strain rates for a differential stress of 100 MPa. Experimental data from the studies of Gleason and Tullis (1995) and Luan and Paterson (1992), as well as the estimated deformation conditions in the Ruby Gap duplex are also shown. The experimental data are normalized to a differential stress of 100 MPa using a stress exponent, n=4. **a** Extrapolation with no correction for the influence of water fugacity on strain rate. **b** Extrapolation with strain rate normalized to a water fugacity of 37 MPa using a water fugacity exponent, m=1

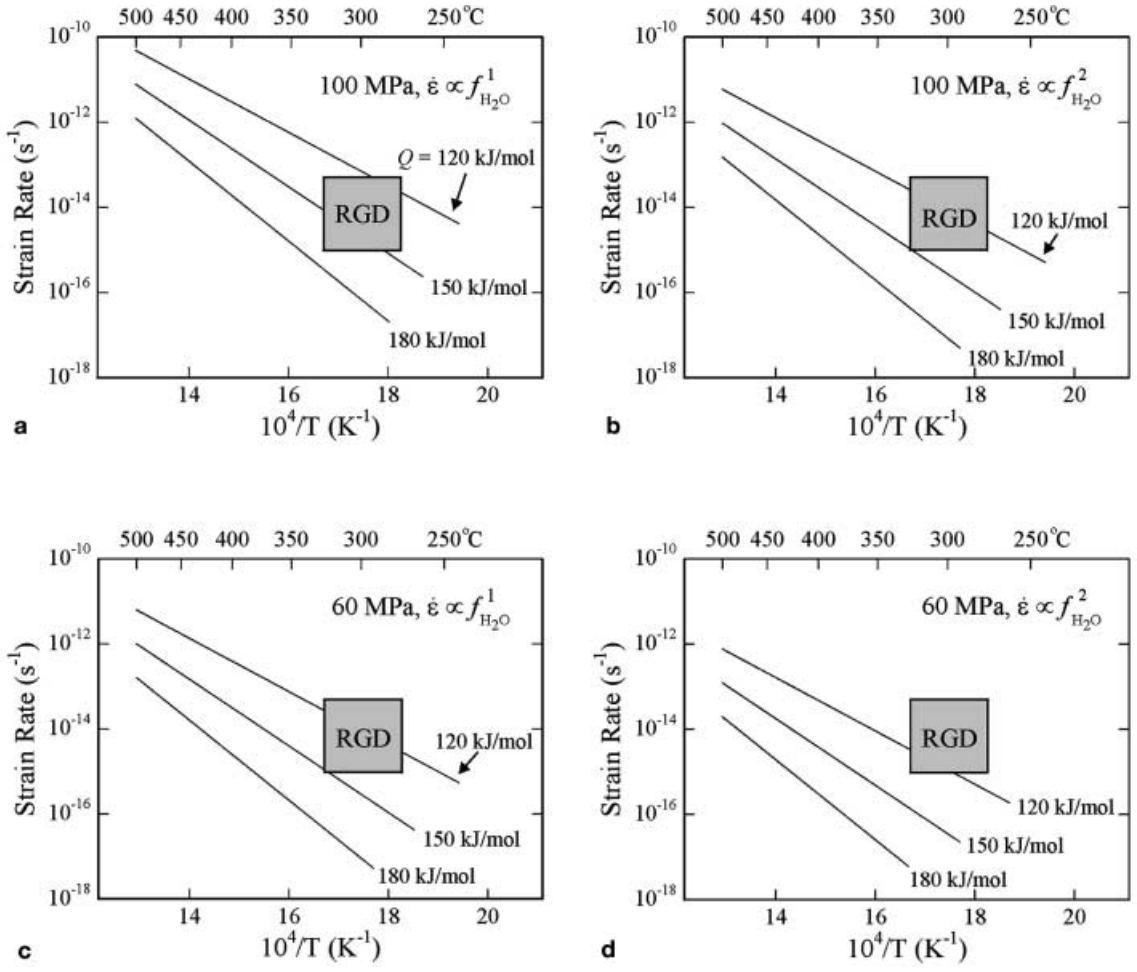

Fig. 4 Log strain rate versus 1/T plots showing extrapolation of experimental flow laws to natural conditions. **a** Same as Fig. 3a; **b** differential stress normalized to 60 MPa using n=4, water fugacity normalized to 37 MPa using m=1; **c** stress normalized to 100 MPa using n=4, water fugacity normalized to 37 MPa using m=2; **d** stress normalized to 60 MPa using n=4, water fugacity normalized to 37 MPa using m=2

sure effect on water fugacity (see Kohlstedt et al. 1995). A narrower range of flow law parameters can then be determined by making the additional assumption that the same flow law describes the deformation of the L&P experiments, the G&T experiments and the mylonites from the Ruby Gap duplex. Strain rates predicted by extrapolating f_{H_2O}-corrected quartzite flow laws to conditions appropriate for the Ruby Gap duplex are shown for differential stresses of 60 and 100 MPa in Figs. 3b and 4. In Fig. 3b the experimental data are normalized to f_{H_2O} =37 MPa using m=1.

One of the largest uncertainties implicit in constructing these plots is the water fugacity in the experiments of G&T. All of the experiments of G&T were conducted on "as-received" samples. Numerous experimental observations indicate that there is sufficient water in these "as-received" samples to significantly enhance the creep rates relative to those observed at dry conditions, however, further weakening is observed by adding additional water (e.g., Jaoul et al. 1984; Kronenberg and Tullis 1984). These observations indicate that at the highest pressures tested, the quartzite samples deformed by G&T may have been undersaturated with water, and therefore the water fugacity is not well constrained. By contrast, free water was present during the deformation experiments of L&P. Assuming that $\dot{\varepsilon} \propto f^1_{H_2O}$, the difference in strain rate between the G&T and L&P data sets illustrated in Fig. 3a is consistent with a f_{H_2O} ≈2500 MPa in the experiments of G&T with f_{H_2O} ≈300 MPa for the experiments of L&P. Similarly, if $\dot{\varepsilon} \propto f^2_{H_2O}$, the difference between the two data sets indicates f_{H_2O} ≈800 MPa for the experiments of G&T. The values of A in Eq. (1) used for extrapolating the flow laws with different values of Q and m were calculated using these values of water fugacity. In equation form, A was calculated by making the assumption that

$$\dot{\varepsilon}_{L\&P} = \dot{\varepsilon}_{G\&T}\Big|_{f_{H_2O(L\&P)}} = A\left(f_{H_2O(L\&P)}/f_{H_2O(G\&T)}\right)^m \sigma^n \exp(-Q/RT) \qquad (2)$$

where $\dot{\varepsilon}_{G\&T}|_{f_{H_2O(L\&P)}}$ is the strain rate of the data of G&T normalized to the water fugacity of the experiments of L&P.

Constraints on the value of the activation energy (Q)

The relatively low strain rates experienced by the duplex, and therefore low temperatures during deformation, enhances our ability to resolve the most acceptable values of Q (subject to the assumptions outlined above) because of the large extrapolation from experimental temperatures. For all conditions considered, the activation energy for creep must be at the lower end of the experimental uncertainty to be consistent with the deformation conditions estimated for the Ruby Gap duplex. As illustrated in Figs. 3b and 4a, assuming $\dot{\varepsilon} \propto f_{H_2O}^1$ and a differential stress of 100 MPa, Q must be in range of ~130–160 kJ/mol to give strain rates in the range of 10^{-14}–10^{-15}/s at ~300 °C. At lower stresses, the best fitting Q becomes significantly less than 150 kJ/mol (Fig. 4c). There is no reasonable set of $\sigma - f_{H_2O}$ conditions that is consistent with a value of Q in the range of 220 kJ/mol.

Similar to the trade-off between stress and activation energy, the best fitting Q values decrease the greater the dependence of water fugacity becomes. As illustrated in Fig. 4b, with values of m=2, the best fitting Q's are again significantly lower than 150 kJ/mol. A more extreme case is illustrated in Fig. 4d, where Q must be lower than ~130 kJ/mol to be consistent with the estimated deformation conditions in the Ruby Gap duplex. If the water fugacity is lower than 37 MPa, because of the presence of other fluids and/or sublithostatic pore-fluid pressures (e.g., Küster and Stöckhert 1999), the activation energy would have to be even lower to be consistent with the deformation conditions in the duplex (and the assumptions outlined above).

Evaluation of experimental constraints on the value of the water fugacity coefficient (m)

Detailed microphysical models for how water influences the rheological properties of quartz are still being developed (e.g., Paterson 1989; Kronenberg 1994). However, experimental observations ranging from the measurement of oxygen diffusion rates (Farver and Yund 1991), the influence of pressure and fluid composition on the rate of dislocation recovery under fluid saturated conditions (Tullis and Yund 1989; Post et al. 1996), and the analysis of rheological data where microstructural observations suggest that dislocation climb controls creep rate (Gleason and Tullis 1995; Kohlstedt et al. 1995; Post et al. 1996) are all consistent with a model in which diffusion rates are enhanced by the presence of a defect in the quartz structure whose concentration increases with increasing water fugacity. These observations all support Paterson's (1989) suggestion to include the water fugacity term in the flow law. Motivated by the trade-off between the best fitting activation energy and water fugacity exponent illustrated in Fig. 4, we now evaluate some of the laboratory constraints on the dependence of water fugacity on creep rate.

Several observations suggest that the water fugacity of G&T's experiments was on the higher side (i.e., near ~2500 MPa, consistent with $\dot{\varepsilon} \propto f_{H_2O}^1$) than the lower side (i.e., ~800 MPa, consistent with $\dot{\varepsilon} \propto f_{H_2O}^2$) of the values used in Fig. 4. First, the strength of "as-received" samples deformed in the molten salt cell at $\dot{\varepsilon} = 1.5 \times 10^{-5}\ s^{-1}$, T=900 °C is lower at a confining pressure of 1,500 MPa than at 1,000 MPa (Gleason and Tullis, 1995); these are the data that G&T used to calculate $\dot{\varepsilon} \propto f_{H_2O}^1$. This observation suggests that there is more than enough water to saturate the quartzite at a pressure of 1000 MPa (where $f_{H_2O} \approx 1800$ MPa), otherwise there is no explanation for why the strength would decrease with increasing pressure. Second, the strength of G&T's "as-received" samples deformed at a confining pressure of 1500 MPa is actually slightly lower than that reported for "water-added" samples (Post et al. 1996) deformed under the same conditions using solid salt as a confining medium (Fig. 5). At the high temperatures employed by Gleason and Tullis (1995), it is possible that water liberated by dehydration of the minor amounts of phyllosilicates in the quartzites provides the additional source of water required to promote "water-added" behavior. There is a greater uncertainty in stress for the experiments conducted using solid salt. However, the results of Gleason and Tullis (1993) indicate that there is little difference in the strength measured for "as-received" samples deformed using solid salt or molten salt at high (i.e., 900–1000 °C) temperatures.

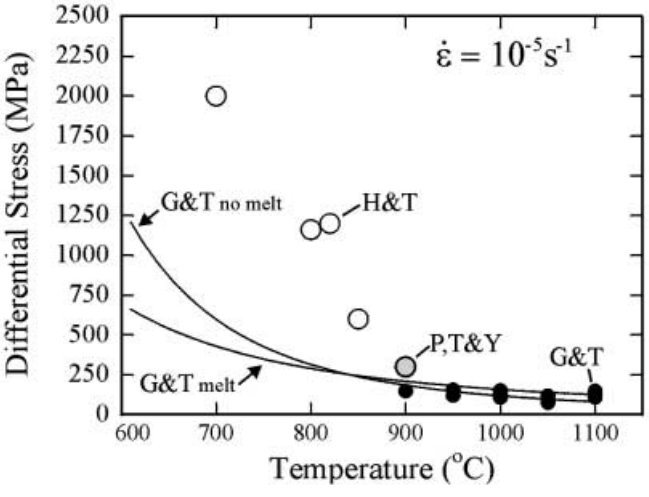

Fig. 5 Plot of temperature versus differential stress for a strain rate of 1.5×10^{-5}/s showing that strengths at lower temperature are significantly underestimated by extrapolation of Gleason and Tullis' (1995) high-temperature flow laws. Experimental data from Gleason and Tullis (1995) (experiments conducted at a confining pressure of 1.5 GPa, labeled G&T), Post et al. (1996) (1.7 GPa, labeled P,T&Y), and Hirth and Tullis (1994) (labeled H&T) are also shown. At temperatures below ~800 °C the quartzites deform by semi-brittle flow (Hirth and Tullis 1994)

A comparison of the data of Post et al. (1996) and Heard and Carter (1968) also indirectly suggests that the water fugacity in Gleason and Tullis' experiments is significantly greater than ~800 MPa. The strength of Post et al.'s (1996) samples deformed at a $\dot{\varepsilon} = 1.5 \times 10^{-5}\ s^{-1}$, T=900 °C and confining pressure of 700 MPa (strength ≈800 MPa) is approximately the same as that measured for Heard and Carter's (1968) "as-received" samples deformed at similar conditions ($\dot{\varepsilon} = 3.6 \times 10^{-5} s^{-1}$, T =900 °C and confining pressure of 800 MPa, strength =710 MPa). This observation suggests that (1) the stress resolution of Post et al.'s experiments is reasonably good, (2) there was enough water present in Heard and Carter's experiments to saturate quartz at these conditions, and (3) the water fugacity in G&T's experiments must be considerably greater than that in Heard and Carter's experiments, as the strength of G&T's samples at the same temperature and strain rate, but higher confining pressure, is significantly lower (~140 MPa at a $\dot{\varepsilon} = 1.5 \times 10^{-5} s^{-1}$, T=900 °C) than that of Heard and Carter's (1968) samples. In summary, this analysis suggests that the water fugacity of G&T's experiments is close to that expected for saturated conditions, and therefore, assuming that the only difference between the data sets of G&T and L&P is the pressure effect on water fugacity, that $\dot{\varepsilon} \propto f^{1}_{H_2O}$.

An evaluation of the effect of temperature on deformation of quartzite at conditions near the transition from regime 2 to regime 1 indicates that the value of m=2 measured by Post et al. (1996) is a result of a change in deformation mechanism with increasing differential stress. Post et al. suggested that the value of m could be overestimated if the large difference in stress observed for high pressure (high f_{H_2O}) and low pressure (low f_{H_2O}) experiments occurs as a result of a change in the rate-limiting step of a serial deformation process. More experimental results are required to analyze this possibility in detail. However, an indication that such a change in deformation mechanism occurs is illustrated in Fig. 5, where the strength of quartzite deformed in regime 1 and in the semi-brittle flow regime (e.g., Hirth and Tullis 1994) is shown to be significantly greater than that predicted by extrapolation of the G&T flow law to lower temperatures. The data shown in Fig. 5 emphasize the importance of determining flow law parameters within a single deformation regime. Indeed, if the analysis of the influence of water fugacity on strain rate is restricted to samples that deformed at stresses less than ~300 MPa, the observed value of m is ~1 [see Gleason and Tullis (1995) and the analysis of the results of Kronenberg and Tullis (1984) presented by Kohlstedt et al. (1995) and Post et al. (1996)].

The increase in strength associated with a transition to regime 1 (Fig. 5) also provides an explanation for the curious result that the stress exponent measured for the coarser-grained "silicic-gel origin" samples of L&P (n=~2.2) is smaller than that determined for the finer-grained "silicic-acid origin" samples. The experimental conditions employed by L&P extended to stresses in the range of 300–500 MPa. The smaller stress exponent observed for the coarse-grained samples could be a manifestation of the transition from climb-controlled to glide-controlled creep. In this case, the measured stress exponent is not representative of a single deformation process. By contrast, the hardening observed with the transition from regime 2 to regime 1 may have been reduced for the fine-grained silicic-acid origin aggregates if a significant amount of recovery was accommodated by grain boundary migration recrystallization (e.g., Tullis and Yund 1985; Hirth and Tullis 1992). Gleason and Tullis (1995) also report an apparent decrease in stress exponent associated with the transition from regime 2 to regime 1.

The Ruby Gap quartzite flow law

The results of the extrapolation of quartzite flow laws to conditions estimated for the Ruby Gap duplex indicate that Q=135±35 kJ/mol with m=1 and n=4. The uncertainty in Q reflects the range in estimated values of the external state variables. Based on the observations described in the previous section we concur with previous analyses (Gleason and Tullis 1995; Kohlstedt et al. 1995; Post et al. 1996) that the value of m=1 provides the best fit to experimental data at stresses less than ~300 MPa (i.e., at stresses below that at the transition between regimes 1 and 2). The uncertainty in the value of Q determined by our analysis is within the reported error of that calculated for L&P's silicic-gel origin flow law and both G&T's flow laws. Additional support for a lower activation energy (i.e., ~135 kJ/mol) is provided by analyzing the conditions where the transitions between the different dislocation creep regimes occur in the laboratory. As illustrated in Fig. 2, the boundaries between the dislocation creep regimes are better defined using G&T's lower activation energy, "melt-present" flow law (Q=137±34 kJ/mol), then the "melt-free" flow law (Q=223±56).

Further refinement of the flow law parameters can be realized by assuming that a single quartzite flow law is appropriate for the complete range of deformation conditions that prevailed during formation of the duplex. The entire suite of dislocation creep microstructures illustrated in Fig. 1 must have been created at conditions within the bounds estimated in the previous section. As illustrated by Dunlap et al. (1997), the differential stress estimated using grain size piezometry for samples from the duplex ranges from ~25 to >200 MPa. Some samples have recrystallized grain sizes indicating stresses as low as ~10 MPa, but these display microstructures indicative of post-deformational grain growth (see Fig. 6f of Dunlap et al. 1997). The highest stresses are calculated for samples that exhibit regime 1 microstructures.

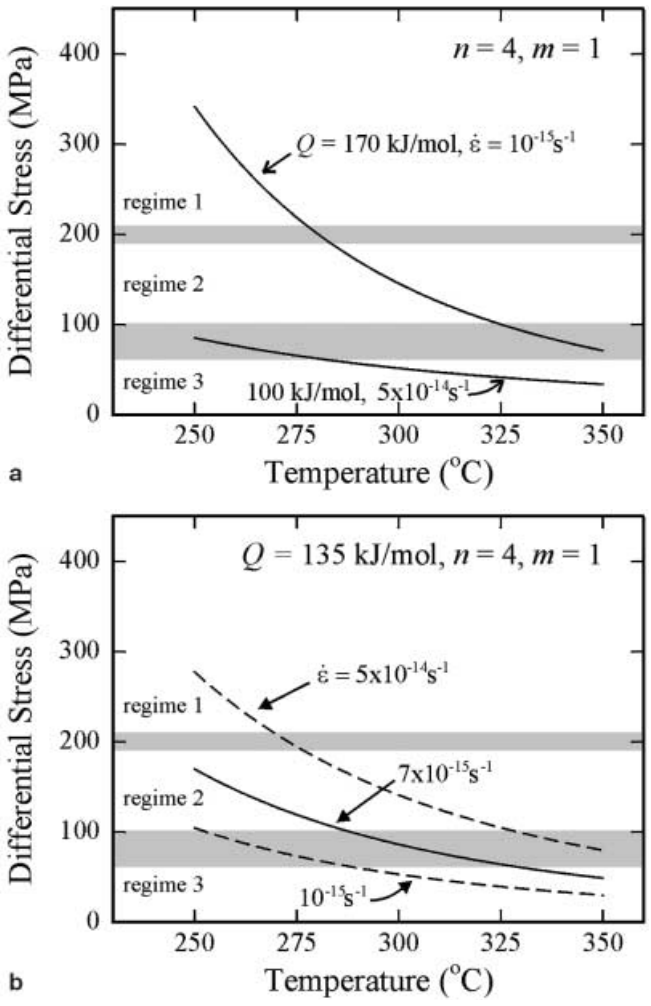

Fig. 6 Plot of temperature versus differential stress illustrating the range of deformation conditions predicted for best fitting quartzite flow law parameters shown in Fig. 4. In both figures the estimated stresses at the transitions between the dislocation creep regimes are shown by the *shaded regions*. Differential stresses were calculated using values of n=4 and m=1. **a** Microstructural observations indicate that the differential stress during the formation of the duplex ranged between <50 and ~200 MPa. Using the most extreme estimates for the activation energy (100 or 170 kJ/mol), this range of differential stress can not be achieved using a single flow law within the deformation conditions estimated for the duplex. **b** With an activation energy of 135 kJ/mol, the entire spectrum of differential stresses can be achieved within the estimated deformation conditions

Within the range of strain rate and temperature estimated for the Ruby Gap duplex, flow laws incorporating the more extreme values of Q are not consistent with the range of differential stresses exhibited. As shown in Fig. 6a, with the lower value of Q (100 kJ/mol), the stress predicted for the lowest temperature and highest strain rates estimated for the duplex is ~80 MPa. Similarly, using the higher value for Q (170 kJ/mol), the stress predicted for the highest temperature and lowest strain rate estimated for the duplex is ~80 MPa. By contrast, the range in stress predicted using Q=135 kJ/mol is large enough to produce the full spectrum of dislocation creep microstructures observed in the duplex within the estimated limits of temperature and strain rate (Fig. 6b). By applying this additional constraint we arrive at a quartzite flow law with parameters $\log(A)$=–11.2± 0.6 MPa^{-n}/s, Q =135±15 kJ/mol, for m=1, and n=4. It is encouraging that this set of flow law parameters also fits the estimated deformation conditions described by Stöckhert et al. (1999) for quartzite deformed in the Italian Alps.

Summary

The similarity of dislocation creep microstructures produced during laboratory experiments and those preserved in naturally deformed quartz mylonites indicates that the same deformation processes operate at geological and experimental conditions. The observation of microstructures characteristic of the different dislocation creep regimes in quartz mylonites from the Ruby Gap duplex, together with the well constrained deformation conditions and the relatively simple deformation history of the duplex, provide the opportunity to test the applicability of different quartzite flow laws at natural conditions. By assuming that the same flow law must satisfactorily describe the rheology of quartzite in both the laboratory and during the formation of the Ruby Gap duplex, we have obtained a quartzite flow law $\dot{\varepsilon} = A f_{H_2O}^m \sigma^n \exp(-Q/RT)$ with values of $\log(A)$ =–11.2±0.6 MPa^{-n}/s and Q=135± 15 kJ/mol, for m=1, and n=4; the values of m and n are constrained by the highest resolution experimental data. The results of our study emphasize the importance of combining observations from both laboratory and geological studies to understand the rheological properties of the crust. The continued improvement of flow laws provided by such studies increases the potential impact of the wide range of theoretical/numerical studies that require knowledge of the rheological structure of the continental crust and lithosphere.

Acknowledgements The results of this study were originally presented at the Rheology and Deformation Mechanism conference held in Basel in 1997. We thank both the convenors of that conference (S. Schmid, R. Heilbronner, and H. Stünitz) and the convenors of the conference in Neustadt (G. Dresen and M. Handy) for continuing a great tradition. We are also grateful for the numerous great conversations we have had with Jan Tullis on the rheology of quartzite. This paper would never have been written without the work she and her students and colleagues have done over the years. We would also like to thank Renee Heilbronner, Holger Stünitz and Michael Stipp for many helpful discussions during the final stages of development of this project, and Bernhard Stöckhert and Chris Spiers for thoughtful reviews of the submitted manuscript. Greg Hirth was funded by NSF grant EAR-9726125 and the Keck Geodynamics program at WHOI. We also offer a belated thank you to Ann Mulligan for her help in collecting samples in the Ruby Gap duplex.

References

Bailey JE, Hirsch PB (1962) The recrystallization process in some polycrystalline materials. Proc R Soc Lond A267:11–30

Brace WF, Kohlstedt DL (1980) Limits on lithospheric stress imposed by laboratory experiments. J Geophys Res 85:6248–6252

Carter NL, Christie JM, Griggs DT (1964) Experimental deformation and recrystallization of quartz. J Geol 72:687–733

De Bresser JHP, ter Heege JH, Spiers CJ (2000) Grain size reduction by dynamic recrystallization: can it result in major rheological weakening? Int J Earth Sci (this issue)

Derby B, Ashby MF (1987) On dynamic recrystallization. Scripta Met 21:879–884

Dresen G, Duyster J, Stöckhert B, Wirth R, Zulauf G (1997) Quartz dislocation microstructure between 7000 m and 9100 m depth from the Continental Deep Drilling Program KTB. J Geophys Res 102:18443–18452

Dunlap WJ (1991) Structure, kinematics and Cooling history of the Arltunga Nappe Complex, central Australia. PhD Thesis, Univ Minnesota, Minneapolis

Dunlap WJ (1997) Neocrystallization or cooling? $^{40}Ar/^{39}Ar$ ages of white micas from low grade mylonites. Chem Geol 143:181–203

Dunlap WJ, Teyssier C, McDougall I, Baldwin S (1992) Ages of deformation from $^{40}Ar/^{39}Ar$ dating of white micas. Geology 19:1213–1216

Dunlap WJ, Teyssier C, McDougall I, Baldwin S (1995) Thermal and structural evolution of the intracratonic Arltunga Nappe Complex, central Australia. Tectonics 14:1182–1204

Dunlap, WJ, Hirth G, Teyssier C (1997) Thermomechanical evolution of a ductile duplex. Tectonics 16:983–1000

Farver JR, Yund RA (1991) Oxygen diffusion in quartz: dependence on temperature and water fugacity. Chem Geol 90:55–70

Freed AM, Lin J (1998) Time-dependent changes in failure stress following thrust earthquakes. J Geophys Res 103:24393–24409

Fry N (1979) Random point distributions and strain measurement in rocks. Tectonophysics 60:89–105

Gleason GC, Tullis J (1993) Improving flow laws and piezometers for quartz and feldspar aggregates. Geophys Res Lett 20:2111–2114

Gleason GC, Tullis J (1995) A flow law for dislocation creep of quartz aggregates determined with the molten salt cell. Tectonophysics 247:1–23

Hacker BR, Yin A, Christie JM, Snoke AW (1990) Differential stress, strain rate, and temperatures of mylonitization in the Ruby Mountains, Nevada: implications for the rate and duration of uplift. J Geophys Res 95:8569–8580

Hames WE, Bowring SA (1994) An empirical evaluation of the argon diffusion geometry in muscovite. Earth Planet Sci Lett 124:161–169

Heard HC, Carter NL (1968) Experimentally induced "natural" intragranular flow in quartz and quartzite. Am J Sci 266:1–42

Hirth G, Tullis J (1992) Dislocation creep regimes in quartz aggregates. J Struct Geol 14:145–159

Hirth G, Tullis J (1994) The brittle–plastic transition in experimentally deformed quartz aggregates. J Geophys Res 99:11731–11747

Hirth G, Dunlap JW, Teyssier C (1998) Dislocation creep regimes in naturally formed quartz aggregates, in Atlas of mylonitic and fault-related rocks. In: Snoke JW, Tullis J, Todd VR (eds) Princeton University Press, Princeton, pp 500–501

Hobbs BE, Ord A, Teyssier C (1986) Earthquakes in the ductile regime? Pageophysics 124:309–336

Jaoul O, Tullis J, Kronenberg A (1984) The effect of varying water contents on the creep behavior of Heavitree quartzite. J Geophys Res 89:4298–4312

Kohlstedt DL, Weathers MS (1980) Deformation induced microstructures, paleopiezometers, and differential stresses in deeply eroded fault zones. J Geophys Res 85:6269–6285

Kohlstedt DL, Evans B, Mackwell SJ (1995) Strength of the lithosphere: constraints imposed by laboratory experiments. J Geophys Res 100:17587–17602

Kronenberg A (1994) Hydrogen speciation and chemical weakening of quartz. In: Heaney PJ (ed) Silica: physical behavior, geochemistry and material applications. Rev Mineral 29:123–176

Kronenberg A, Tullis J (1984) Flow strengths of quartz aggregates: grain size and pressure effects due to hydrolytic weakening. J Geophys Res 89:42981–4297

Küster M, Stöckhert B (1999) High differential stress and sublithostatic pore fluid pressure in the ductile regime – microstructural evidence for short-term post-seismic creep in the Sesia Zone, Western Alps. Tectonophysics 303:263–277

Law RD, Knipe RJ, Dayan H (1984) Strain path partitioning within thrust sheets: microstructural and petrofabric evidence from the Moine Thrust zone at Loch Eriboll, northwest Scotland. J Struct Geol 6:477–497

Lister GS, Snoke AW (1984) S-C mylonites. J Struct Geol 6:617–638

Luan FC, Paterson MS (1992) Preparation and deformation of synthetic aggregates of quartz. J Geophys Res 97:301–320

McLaren AC, Hobbs BE (1972) Transmission electron microscope investigation of some naturally deformed quartzites. In: Heard HC, Borg IY, Carter NL, Raleigh CB (eds) Flow and fracture of rocks. Am Geophys Monogr 16:55–66

Ord A, Christie JM (1984) Flow stresses from microstructures in mylonitic quartzites of the Moine Thrust zone, Assynt area, Scotland. J Struct Geol 6:639–654

Paterson MC (1989) The interaction of water with quartz and its influence in dislocation flow – an overview. In: Karato S-I, Toriumi M (eds) Rheology of solids and of the Earth. Oxford University Press, Oxford, pp 107–142

Paterson MS, Luan FC (1990) Quartzite rheology under geological conditions. In: Knipe RJ, Rutter EH (eds) Deformation mechanisms, rheology and tectonics. Geol Soc Spec Publ 54:299–307

Post AD, Tullis J (1999) A recrystallized grain size piezometer for experimentally deformed feldspar aggregates. Tectonophysics 303:159–173

Post AD, Tullis J, Yund RA (1996) Effects of chemical environment on dislocation creep of quartzite. J Geophys Res 101:22143–22155

Purdy JW, Jager E (1976) K–Ar ages on rock-forming minerals from the Central Alps. Mem Inst Geol Mineral Univ Padova 30:1–34

Shimamoto T, Ikeda Y (1976) A simple algebraic method for strain estimation from deformed ellipsoidal objects. 1. Basic theory. Tectonophysics 36:315–337

Shimizu I (1998) Stress and temperature dependence of recrystallized grain size: a subgrain misorientation model. Geophys Res Lett 25:4237–4240

Sibson RH (1977) Fault rocks and fault mechanisms. J Geol Soc Lond 133:191–213

Stipp M, Heilbronner R, Stunitz H (1999) Dislocation creep microstructures as indicators of deformation conditions; microstructural analysis of field examples. Abstracts Programs – Geol Soc Am 31:109

Stöckhert B, Brix MR, Kleinschrodt R, Hurford AJ, Wirth R (1999) Thermochronometry and microstructures of quartz – a comparison with experimental flow laws and predictions on the temperature of the brittle–plastic transition. J Struct Geol 21:351–369

Tödheide K (1972) Water at high temperature and pressure. In: Franks F (ed) Water: a comprehensive treatise. pp 463–514

Tullis J, Yund RA (1985) Dynamic recrystallization of feldspar: a mechanism for ductile shear zone formation. Geology 13:238–241

Tullis J, Yund RA (1989) Hydrolytic weakening of quartz aggregates: the effects of water and pressure on recovery. Geophys Res Lett 16:1343–1346

Tullis J, Christie JM, Griggs DT (1973) Microstructures and preferred orientations of experimentally deformed quartzites. Geol Soc Am Bull 84:297–314

Twiss RJ (1977) Theory and applicability of recrystallized grain size paleopiezometer. Pageophysics 115:227–244

White S (1976) The effects of strain on the microstructure, fabrics, and deformation mechanisms in quartz. Philos Trans R Soc Lond A283:69–86